

New Synthetic Routes to Triazolo-benzodiazepine Analogues: Expanding the Scope of the Bump-and-Hole Approach for Selective Bromo and Extra-Terminal (BET) Bromodomain Inhibition

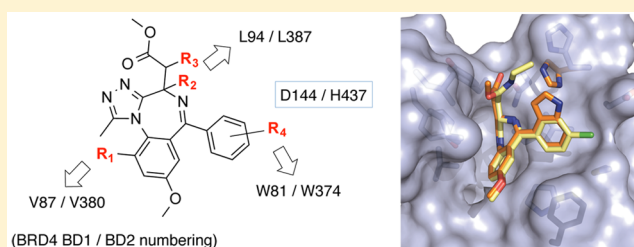
Matthias G. J. Baud,^{†,‡,||} Enrique Lin-Shiao,^{†,‡,⊥} Michael Zengerle,[†] Cynthia Tallant,^{‡,§} and Alessio Ciulli^{*,†,‡}

[†]Division of Biological Chemistry and Drug Discovery, College of Life Sciences, University of Dundee, James Black Centre, Dow Street, Dundee DD1 5EH, U.K.

[‡]Department of Chemistry, University of Cambridge, Lensfield Road, Cambridge CB2 1EW, U.K.

Supporting Information

ABSTRACT: We describe new synthetic routes developed toward a range of substituted analogues of bromo and extra-terminal (BET) bromodomain inhibitors I-BET762/JQ1 based on the triazolo-benzodiazepine scaffold. These new routes allow for the derivatization of the methoxyphenyl and chlorophenyl rings, in addition to the diazepine ternary center and the side chain methylene moiety. Substitution at the level of the side chain methylene afforded compounds targeting specifically and potently engineered BET bromodomains designed as part of a bump and hole approach. We further demonstrate that marked selectivity for the second over the first bromodomain can be achieved with an indole derivative that exploits differential interaction with an aspartate/histidine conservative substitution on the BC loop of BET bromodomains.



INTRODUCTION

The 1,4-benzodiazepine scaffold occupies a place of choice in the toolbox of medicinal chemists and is often referred to as a “privileged scaffold” in drug discovery. A large number of biologically active small molecules containing a 1,4-benzodiazepine scaffold have been approved by the FDA for the treatment of various disease states, although most of them are well-known for their psychotropic effects.¹ Well known examples include diazepam, alprazolam or prazepam. The therapeutic potential of 1,4-benzodiazepines has fueled the interest of synthetic chemists in developing new routes to a range of substituted analogues for biological evaluation.^{2–4} Recently, this scaffold has attracted particular attention in the field of epigenetics, with the discovery of a class of potent small molecule inhibitors of the interaction between Bromo and Extra-Terminal (BET) bromodomain proteins and their acetylated histone substrates. BET proteins Brd2, Brd3, Brd4, and Brdt are key transcriptional co-regulators. Crucial to their activity are paired and highly homologous bromodomains located in their amino-terminal regions. The individual function of the first bromodomain (e.g., Brd2(1)) versus second bromodomain (e.g., Brd2(2)) of BET proteins is however unclear. A number of BET bromodomain inhibitors are currently in clinical trials for the treatment of cancer,⁵ including representative molecules I-BET762 (1),⁶ JQ1 (2),⁷ GW841819X (3),⁸ OTX015 (4),⁹ and RVX-208 (5)¹⁰ (Figure 1A). In particular, compounds 1–4 are based on a triazolo-aryldiazepine scaffold (aryl = methoxyphenyl or dimethylth-

iophene) and bind to the acetyl-lysine (KAc) pocket of BET bromodomains with high affinity (K_d of 1 = 50–370 nM).¹¹ These compounds display activity *in vivo*¹² against a number of disease states, including NUT-midline carcinoma,¹³ multiple myeloma,¹⁴ mixed-lineage leukemia,¹⁵ and acute myeloid leukemia.^{16,17} Despite selectively targeting the BET bromodomain family with high potency over other bromodomains, these compounds are pan-BET selective thus do not significantly discriminate between individual bromodomains of the four BET members. This lack of selectivity within the BET subfamily so far has prevented accurate deconvolution of the biological function of individual BET proteins and of their tandem bromodomains. To address this problem, we recently developed a chemical genetics approach to engineer the selectivity of the BET bromodomain inhibitor I-BET762/JQ1 within the BET proteins family.¹¹ This so-called “bump and hole” approach is based on the generation of orthogonal and high-affinity protein/ligand pairs and involves introducing a single point mutation (large to smaller amino acid, that is, the “hole”) onto the BET bromodomain of interest together with making a synthetic modification (bulky substituent, that is, the “bump”) onto the parent BET bromodomain binder to complement the newly created protein subpocket (Figure

Special Issue: Epigenetics

Received: July 20, 2015

Published: September 14, 2015

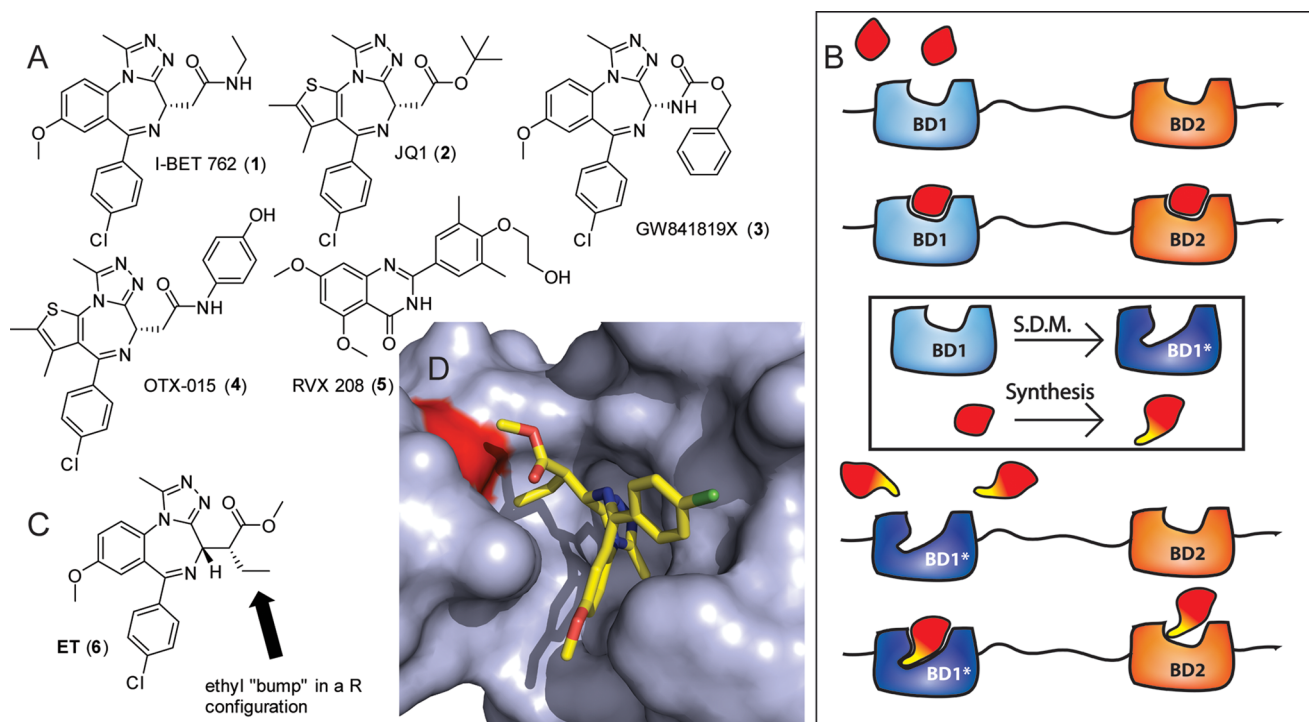


Figure 1. (A) Structures of BET bromodomain probes I-BET762 (1), JQ1 (2), GW841819X (3), OTX-015 (4), and RVX-208 (5), currently in clinical trials, (B) bump and hole approach to engineer the selectivity of BET bromodomain probes against individual BET bromodomains, (C) structure of ET (6), and (D) cocrystal structure of Brd2(2)_{L383A} (blue, surface representation) in complex with ET (6) (stick representation, yellow carbons), PDB code 4QEW.¹¹ The L/A mutation is shown in red.

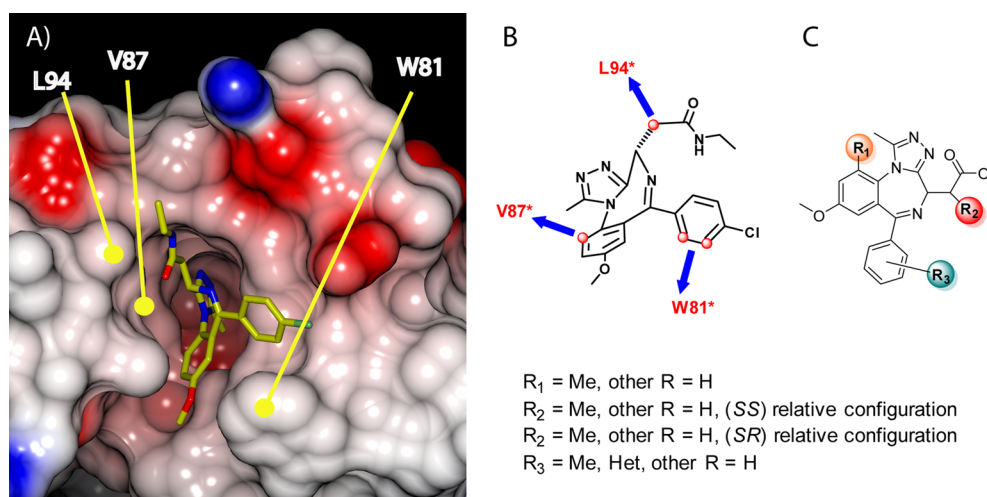
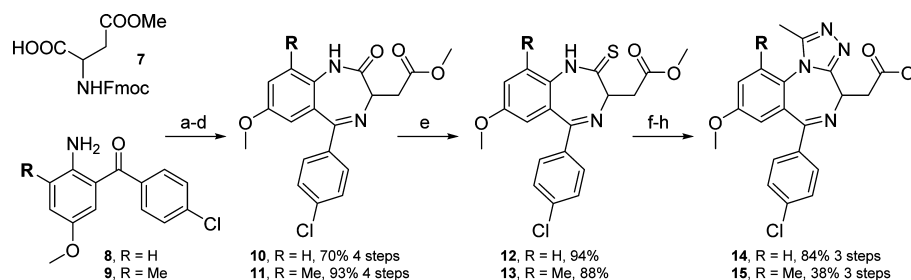


Figure 2. (A) Crystal structure of I-BET762 (1, yellow carbons) bound to Brd4(1) (PDB code 3P5O,² surface representation; red indicates negative and blue positive electrostatic potential). W81, V87, and L94 are highlighted. (B, C) I-BET762 chemical structure and positions selected for derivatization to target the corresponding mutations.

1B). As a result, the bulky ligand is expected to bind with high affinity to the mutated BET protein, while exhibiting weak to no binding to wild-type (WT) proteins due to a steric clash occurring between the “bump” and the naturally occurring residue (Figure 1B). This approach was previously shown to aid selective targeting of protein kinases through engineering of the ATP binding site and ATP cofactor as well as ATP-competitive inhibitors.^{18,19} In our study, we demonstrated for the first time that the bump and hole approach can be used to selectively disrupt protein–protein interactions within the BET family of proteins.¹¹ Compound ET (6) (Figure 1C,D), a derivative of I-BET762/JQ1 bearing an ethyl functional group at the level of

the side chain methylene moiety, bound to leucine/alanine mutant BET bromodomains with low nanomolar affinity and displayed up to 540-fold and no less than 40-fold (160-fold on average) selectivity relative to WT BET bromodomains across the entire subfamily. This orthogonal bromodomain/ligand pair was used within cancer cells to show that selective blockade of the first bromodomain of a given BET protein, Brd4, is sufficient to displace it from chromatin.¹¹ The exquisite selectivity provided by ET for engineered bromodomains is currently exploited in our laboratory to probe the biology of individual BET proteins through selective modulation of their interaction with their histone substrates. Selective modulation

Scheme 1. Synthesis of 14 and Its Methylated Derivative 15^a

^aConditions: (a) SOCl_2 , CH_2Cl_2 , reflux, 2.5 h; (b) benzophenone, CHCl_3 , reflux, 3 h; (c) Et_3N , CHCl_3 , reflux, 16 h; (d) AcOH , 1,2-DCE, 60 °C, 3 h; (e) Lawesson's reagent, toluene, reflux, 4 h; (f) hydrazine- H_2O , THF, 0 °C, 5 h; (g) AcCl , Et_3N , 0 °C to rt, 16 h; (h) AcOH , rt, 2 days (R = H) or reflux, 3 h (R = Me).

of individual BET bromodomains is important for accurate and reliable target validation in the different disease states that are associated with unbalanced activity of BET proteins.

The ET-L/A orthogonal inhibitor–protein pair was discovered and optimized within the framework of an extended study in which we explored several mutations (“holes”) and I-BET762 substitution patterns (“bumps”). In the current manuscript, we report the full journey that led to that discovery. In doing so, we also describe our synthetic efforts toward **6** and other novel analogues aimed at targeting the mutant proteins. In particular, we report new synthetic routes that we developed toward this aim, including I-BET762 analogues bearing substitution patterns at the level of the methoxyphenyl and chlorophenyl rings, in addition to the side chain methylene. Finally, we present biophysical evaluation of the compounds within the context of our bump-and-hole project, and highlight useful isoform selectivity criteria for the design of the next generation of BET bromodomain inhibitors.

RESULTS AND DISCUSSION

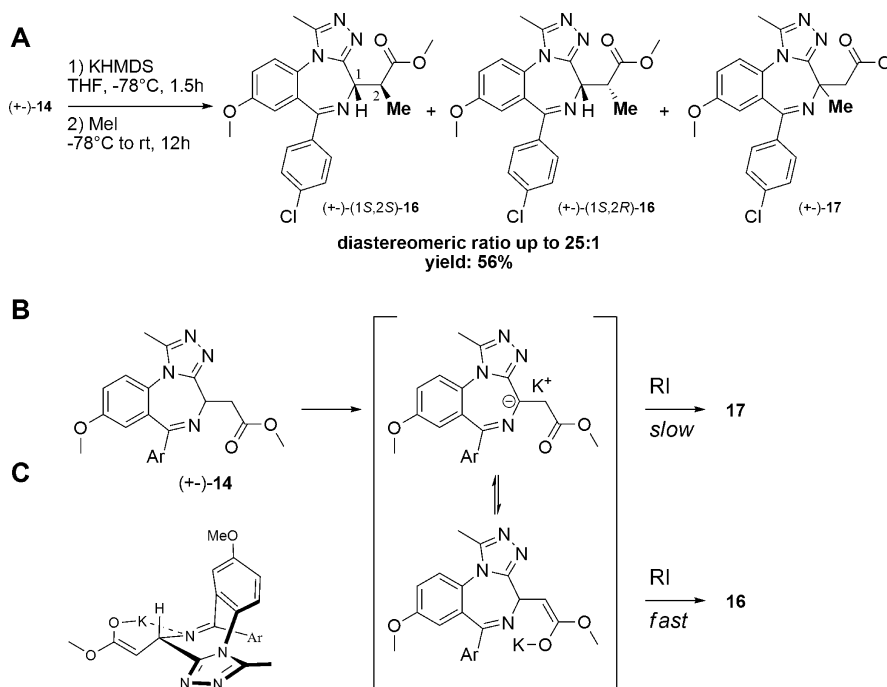
Design of Engineered BET Bromodomain–Ligand Pairs and Synthetic Targets. Analyses of sequence alignments (Figure S1) and inhibitor-bound crystal structures¹¹ guided us to focus on 11 residues that are strictly conserved within the BET subfamily and are in close contact with the ligand. Keeping in mind that the introduced mutations should not significantly disrupt protein stability and substrate binding, residues Y97, C136, Y139, and N140 (Brd4(1) numbering) were discarded, because they are known to be important for KAc recognition^{20–25} and for preserving a key network of bound water molecules.²⁶ Buried residues P82 and F83 from the bottom of the so-called WPF shelf were also discarded because their mutation was predicted to destabilize the integrity of the hydrophobic core.²¹ Residues L92 and M149 looked promising but were not pursued further due to a lack of suitable vectors arising from the inhibitor scaffold that could be exploited to complement potential mutations. The remaining three residues, that is, the more peripheral hydrophobic W81 from the top of the WPF shelf and V87 and L94 from the ZA loop, were selected for site directed mutagenesis (Figure 2A). Mutants W/F, W/H, V/A, L/I, and L/A were constructed within Brd2(1), recombinantly expressed, purified from *Escherichia coli* and biophysically characterized in order to assess their stability and histone binding capacity (Table S1). All mutants maintained melting temperatures (T_m) above 37 °C, and most had comparable stabilities to the WT proteins, as assessed by differential scanning fluorimetry (DSF). Importantly,

all mutants retained competence to bind a tetra-acetylated H4 derived peptide²⁷ as assessed by ITC albeit to varying degrees (Table S1). Most mutants exhibited comparable peptide binding affinities relative to WT, while the V/A proved the most disruptive mutation.

With three positions identified and corresponding mutants characterized, I-BET762 (**1**) was selected as the starting scaffold because it is more synthetically tractable and better suited to all required vectors than JQ1. Molecular modeling studies suggested that (i) a “bump” R_1 originating from the methoxyphenyl ring could target the hole introduced by the V87A mutation, (ii) R_2 functionalization at the level of the side chain methylene, in an (*R*) configuration, could target L94 mutations, and (iii) the *p*-chlorophenyl ring could provide suitable vectors for R_3 substituents to explore W81 mutations (Figure 2B,C). A methyl group was elected as the bump of choice to explore the engineered holes because it represents the smallest hydrophobic functional group that at the same time introduces minimal alteration of the ligand scaffold in terms of electronics, conformation, and physicochemical properties. We therefore performed a “methyl scan” around the I-BET762 scaffold by synthesizing analogues functionalized with methyl groups at R_1 – R_3 (Figure 2C) to target mutations at the respective positions.

Chemical Strategies To Target the V87A Mutation: R_1 = Me. The ester derivative of I-BET762 was chosen as the parent scaffold for efficient enolate generation and substitution of the methylene side chain (R_2 , see later). Compound **14** was prepared as previously described, with significant yield improvement (55% overall) compared with those reported by Chung et al. (22% overall) (Scheme 1).⁸ Chlorination of protected acid **7**²⁸ and N-acylation of the appropriate amino-benzophenones **8** and **9**, followed by Fmoc deprotection and subsequent cyclization afforded **10** and **11** in excellent yields in a four-step, one-pot sequence. Further thionation afforded thioamide derivatives **12** and **13**. Treatment of thioamides **12** and **13** with hydrazine monohydrate, followed by acetylation and further cyclization in acidic conditions afforded triazoles **14** and **15** in high yield in a three-step, one-pot procedure. Starting from benzophenone derivative **9** allowed us to ultimately introduce the R_1 methyl group (Figure 2C). While yields for the condensation and thionation reactions were excellent, the triazole formation toward **15** proceeded in only 38% yield, much lower than in the case of **14**. This reflects the lower yield for the final cyclization (Scheme 1, step h), which only proceeded under reflux conditions, along with significant degradation. We attributed the latter to the steric demand

Scheme 2. (A) Alkylation of (\pm)-14 Providing a Mixture of Diastereomers and Alkylation at C1, (B) Proposed Overall Mechanism for the Observed Results, and (C) Proposed Transition State for the Enolate Alkylation

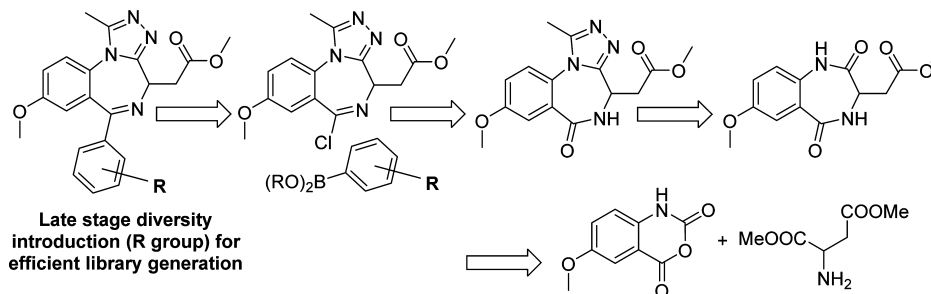
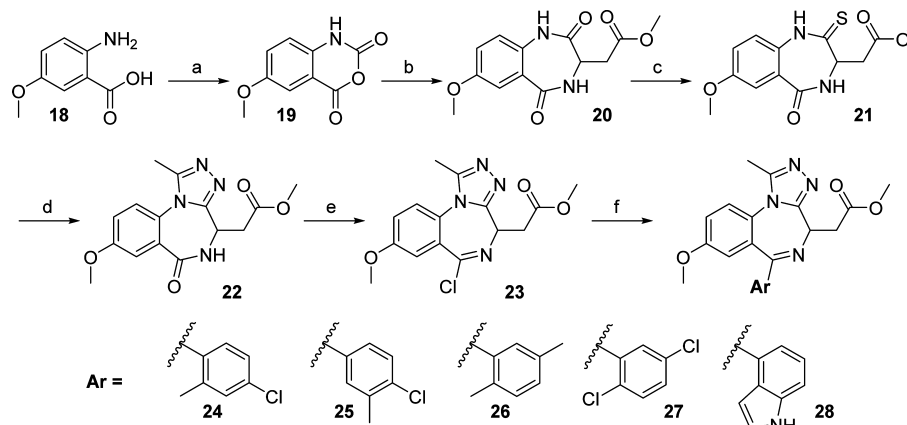


imposed by the R_1 methyl group and the triazole methyl group in the cyclization process.

Chemical Strategies To Target the L94 Mutations: R_2 = Me. We envisaged that introduction of alkyl substituents on the methylene side chain would be achievable through the generation of the enolate of **14** followed by reaction with an alkyl halide (Scheme 2). Among the various bases explored for enolate generation, including LDA, NaH, and KHMDS, the latter proved the most efficient and provided the cleanest reaction and best yields. Treatment of (\pm)-**14** with 1.2 equiv of KHMDS at -78°C , followed by addition of methyl iodide, afforded a diastereomeric mixture of (\pm)-(1*S*,2*S*)-**16** and (\pm)-(1*S*,2*R*)-**16** (Scheme 2A). The reaction provided (\pm)-(1*S*,2*S*)-**16** as the major alkylation product and proved to be highly diastereoselective, for example, up to 25:1 with MeI. Such selectivity was strongly dependent on the temperature gradient, in certain cases down to 3:1. The structure of the major diastereomer resulting from the alkylation of (\pm)-**14** with MeI could be unambiguously assigned as (\pm)-(1*S*,2*S*)-**16** on the basis of previous crystallographic studies.¹¹ We refer to the active stereomer (\pm)-(1*S*,2*R*)-**16** as **ME** for clarity.¹¹ The reason for this observed diastereoselectivity is unclear. The potassium counterion might provide conformational restriction to the (*Z*)-enolate in a six-membered ring transition state via coordination to the sp^2 nitrogen of the diazepine ring (Scheme 2C). However, in such a transition state the observed preference for the attack on the pro-*S* face is not evident simply based on sterics, suggesting that other factors come into play. Further mechanistic studies will be needed to address this point. Nevertheless, when a high diastereomeric ratio did not allow for the isolation of reasonable amounts of the desired active (\pm)-(1*S*,2*R*)-**16** diastereomer in pure form, the diastereomeric mixture could be readily epimerized with sodium methoxide under microwave irradiation to afford a 1:1 mixture of diastereomers, which could then be separated by flash column chromatography.

Along with alkylation of the side chain, we observed minor albeit observable alkylation of the ternary C1 carbon of the diazepine ring, affording derivative (\pm)-**17**. This suggests that the C1 position of (\pm)-**14** is deprotonated, at least partially, during addition of KHMDS at -78°C . This is consistent with the intense dark color observed following addition of KHMDS, potentially reflecting the generation of a highly delocalized anionic species. During their study of the memory of chirality in related 1,4-benzodiazepin-2-one systems, the Carlier group documented the installment of quaternary centers at C1 using enolate alkylation chemistry.^{29–31} Notably, they also observed superior results when using KHMDS as a base for enolate generation. Due to the “privileged” status attributed to the 1,4-benzodiazepin-2-one scaffold in drug discovery, this represented an important finding because it offered the first short and robust route toward novel, conformationally restricted 1,4-benzodiazepin-2-one analogues.^{29–31} We here show that installment of a quaternary center at C1 on a triazolo-benzodiazepine scaffold can indeed be achieved, although in low yield. This can be particularly attractive if one wants to develop structure–activity relationships of BET bromodomain binders (e.g., **1–4**) through double functionalization at C1. In particular, this would represent a real advantage to the use of quaternary amino acid precursors, which are sterically hindered and likely to reduce the overall yield, in addition to being expensive and providing a narrow scope for substitution. Moreover, this would offer a late state divergent synthetic strategy toward library analogues. However, the usefulness and general applicability of such a strategy will be contingent on more robust reaction conditions and improved yields. Further optimization studies are ongoing in our laboratories in order to tune the regioselectivity, reaction times, and yields of this key reaction. Of note, the ^1H NMR spectrum of (\pm)-**17** showed two species in a ca. 2:1 ratio. This is reflective of the slow conformational equilibrium imposed by the steric demand at C1, in line with Carlier’s results.²⁹

Scheme 3. Proposed retrosynthetic Analysis for the Functionalization of the Chlorophenyl Ring

Scheme 4. Racemic Synthesis of Analogues 24–28^a

^aConditions: (a) triphosgene, THF, rt, quant; (b) Asp-(OMe)₂, pyridine, reflux, 24 h, 42%; (c) Lawesson's reagent, pyridine, reflux, 1.25 h, 48%; (d) AcNHNH₂, Hg(OAc)₂, THF/AcOH, rt, 24 h, 91%; (e) P(O)Cl₃, *N,N*-dimethylaniline, 125 °C, 1 h, 39%; (f) ArB(OH)₂, Et₃N, Pd(PPh₃)₄, DMF, 100 °C, 27–31%.

Chemical Strategies To Target the W81 Mutations: Derivatization of the Chlorophenyl Ring. We envisaged that developing new synthetic routes toward the I-BET scaffold would be of particular interest to gain rapid access to libraries of analogues to address other mutational positions in the binding pocket. Specifically, we next explored the possibility to access I-BET762 analogues with diverse substitution patterns at the level of the chlorophenyl ring (Figure 2C). While this should be potentially achievable through previously reported routes (Scheme 1), the early stage introduction of the chlorophenyl ring makes this linear sequence very impractical for analogue generation. We therefore considered that a new route allowing the late stage introduction of the substituted phenyl moiety would be valuable. We hypothesized that such analogues would be obtained by Suzuki–Miyaura cross coupling of an imidoyl chloride with an appropriate phenylboronic acid derivative³² (Scheme 3). A wide variety of phenylboronic acid derivatives are commercially available, readily accessible, and affordable. The imidoyl chloride would be obtained by chlorination of the corresponding amide. The triazole moiety would in turn be introduced from the corresponding amide, through a thionation/condensation/cyclization sequence. The diamide would be obtained through condensation of inexpensive 5-methoxyisatoic anhydride³³ and aspartic acid dimethyl ester.

The synthesis of our library of analogues is shown in Scheme 4. 2-Amino-5-methoxybenzoic acid **18** was converted to 5-methoxyisatoic anhydride **19** in quantitative yield.³³ Condensation of **19** with aspartic acid dimethylester afforded the bicyclic precursor **20** in 42% yield. Selective thionation could be achieved by treatment with Lawesson's reagent in refluxing

pyridine, affording thioamide **21** in 48% yield. We envisaged that a one-step procedure for the installment of the triazole would be particularly convenient compared with the three-step procedure employed previously (Scheme 1). A representative set of conditions used for the installment of the triazole moiety is shown in Table 1. Reaction outcome was assessed by NMR of crude mixtures. Thioamide **21** was poorly soluble in a variety of solvents but was soluble in refluxing pyridine. Treatment of **21** with 2.5 equiv of acethydrazide for 1 day at reflux led to the formation of product **22**, along with remaining unreacted **21** and significant formation of the exocyclized product arising from condensation of the intermediate acylhydrazone with the

Table 1. Representative Conditions for Triazole Formation (Conversion of **21** to **22**)^a

entry	conditions	outcome
1	2.5 equiv of AcNHNH ₂ , pyridine, reflux ~1 d	mix. 21 (32%) + 22 (43%) + exocyclization (25%)
2	6 equiv of AcNHNH ₂ , pyridine, reflux ~1 d	mix. 21 (22%) + 22 (29%) + exocyclization (49%)
3	3 equiv of AcNHNH ₂ , pyridine, rt, 1 d	21 insoluble
4	3 equiv of AcNHNH ₂ , 1.5 equiv of Hg(OAc) ₂ , pyridine, rt, 1 d	acylhydrazone (>95%) + 22 (<5%)
5	3 equiv of AcNHNH ₂ , 1.5 equiv of Hg(OAc) ₂ , MeCN, rt, 6 d	acylhydrazone (87%) + 22 (13%)
6	3 equiv of AcNHNH ₂ , 1.5 equiv of Hg(OAc) ₂ , THF/AcOH, rt, 24 h	91% 22

^aYields for entries 1–5 were determined based on NMR spectra of crude samples. The yield for entry 6 is for the isolated, purified material.

Table 2. "Methyl Scan"^a

bromodomain protein	I-BET762 (1)	15	16 ^b	ME ^c	24	25	26	27	28
Brd2(1)	5.4 ± 0.5	0.7 ± 0.2	-0.3 ± 0.2	3.2 ± 0.2	6.3 ± 0.1	1.5 ± 0.2	1.8 ± 0.2	1.2 ± 0.2	6.8 ± 0.6
Brd2(1) _{V103A}	0.1 ± 0.6	0.5 ± 0.3							
Brd2(1) _{L110I}	6.7 ± 0.4		0.0 ± 0.5	5.7 ± 0.7					
Brd2(1) _{L110A}	3.1 ± 0.4		1.6 ± 0.2	7.9 ± 0.2					
Brd2(1) _{W097F}	0.4 ± 0.2				1.4 ± 0.2	-0.1 ± 0.2	0.1 ± 0.2	0.0 ± 0.2	1.9 ± 0.5
Brd2(1) _{W097H}	0.7 ± 0.2				0.9 ± 0.3	0.2 ± 0.2	-0.4 ± 0.3	-0.4 ± 0.2	0.6 ± 0.3
Brd2(2)	8.3 ± 0.3	4.0 ± 0.1	0.2 ± 0.2	5.6 ± 0.1	6.6 ± 0.2	3.2 ± 0.1	3.5 ± 0.1	2.5 ± 0.2	7.7 ± 0.2
Brd2(2) _{V376A}	1.1 ± 0.0	1.2 ± 0.1							
Brd2(2) _{L383I}	9.3 ± 0.3		0.3 ± 0.2	9.6 ± 0.1					
Brd2(2) _{L383A}	6.4 ± 0.2		0.8 ± 0.6	9.3 ± 0.2					
Brd2(2) _{W370F}	2.1 ± 0.0				2.8 ± 0.1	1.5 ± 0.0	0.6 ± 0.1	0.3 ± 0.0	5.2 ± 0.1
Brd2(2) _{W370H}	1.7 ± 0.2				1.1 ± 0.2	1.0 ± 0.3	-0.1 ± 0.1	-0.4 ± 0.2	2.7 ± 0.4

^aThermal stabilization (°C) of wild-type and mutant Brd2 bromodomains by I-BET derivatives 15, 16, 24–28, as assessed by DSF. ^b(±)-(1S,2S)-16. ^c(±)-(1S,2R)-16 (ME).

side chain ester (Table 1, entry 1). Increasing the number of equivalents of acetylhydrazide resulted in low formation of 22 and afforded the exocyclized byproduct as the major component of the reaction (Table 1, entry 2). We envisaged that exocyclization could be prevented by lowering the reaction temperature. However, the reaction did not proceed due to the poor solubility of 21 in pyridine at rt (Table 1, entry 3). Despite its poor solubility, activation of the thioamide with thiophilic mercury diacetate³⁴ allowed for rapid and quantitative consumption of 21 at rt and afforded the intermediate acylhydrazone almost quantitatively along with trace amount of product 22 (Table 1, entry 4). Switching the solvent to acetonitrile led to similar results, even after reaction times up to 6 days (Table 1, entry 5). Pleasingly, changing the solvent to THF/AcOH afforded the desired product 22 in 91% yield after 24 h reaction. Other methods involving chlorophosphate reagents have been previously reported for the installment of the triazole unit of JQ1, although in those cases the amide derivatization step required cooling to -78 °C and the subsequent cyclization step required heating up to 90 °C.^{7,35} Despite the toxicity of the mercury reagent, our one-step procedure is particularly convenient because it is milder, lowers the reaction time by ca. 3-fold compared with previously reported routes, does not require intermediate workup, and proceeds smoothly at rt (and even at 0 °C), while displaying similar yields. Of note, this procedure could also be applied for the conversion of 12 to 14 (Scheme 1) with a 91% yield. The amide of 22 was subsequently converted to the corresponding imidoyl chloride 23 in 39% yield. In particular 23 proved to be moisture and nucleophile (e.g., MeOH) sensitive, which translates into the only moderate yield obtained for its formation. Finally, Suzuki–Miyaura cross-coupling of imidoyl chloride 23 with a set of representative phenylboronic acids³² afforded the final substituted I-BET analogues 24–28. As a control, coupling of 23 with 4-chlorophenylboronic acid afforded the parent molecule 12, as compared by ¹H NMR with a reference sample. This synthetic route proved to be robust and reasonably scalable, allowing preparation of imidoyl chloride precursor 23 on a 2 mmol scale after five steps. Of interest, no chromatographic step was required prior to obtaining triazole 22. The poor solubility of 20 and 21 in a variety of solvents allowed them to be isolated in pure form by simple trituration and filtration. Of note, the synthetic routes described here are purposely racemic in order to provide maximum stereochemical diversity. However, nonracemizing

conditions should in theory be applicable to this route. In particular, the use of chlorophosphate reagents instead of Lawesson's reagent or P₂S₅ for triazole formation has been previously shown to significantly reduce epimerization at the level of the ternary center (final dr 9:1).^{7,35}

Biophysical Evaluation. In order to determine which position and substitution combination would provide the best selectivity profile, binding of I-BET762 and analogues 15, (±)-(1S,2S)-16, ME, and 24–28 against WT and mutant Brd2(1) and Brd2(2) proteins was assessed initially by differential scanning fluorimetry (Table 2). Brd2(1) and Brd2(2) were chosen as representatives of the first and second bromodomains of BET proteins, respectively. Introduction of methyl "bumps" at R₁ and R₃ (methoxyphenyl and chlorophenyl rings, respectively, cpds 15 and 24–28) did not provide noticeable thermal stabilization of the targeted Brd2 mutants compared with WT. In contrast, the methyl bump at R₂ in a 2-R configuration (ME) provided the first evidence of selective stabilization in our engineered system.¹¹ Compound ME induced ΔT_m of 5.7 and 9.6 °C on Brd2(1)_{L110I} and Brd2(2)_{L383D} respectively, while stabilizing the WT proteins by only 3.2 and 5.6 °C. This selective thermal stabilization was even more pronounced in the case of the L/A mutations, with ΔT_m of 7.9 and 9.3 °C against Brd2(1)_{L110A} and Brd2(2)_{L383A}, respectively. This selectivity profile was validated by measuring dissociation constants (K_d) using ITC (Table 3). ME was

Table 3. Affinities (K_d's) and Binding Enthalpies (ΔH) Obtained by ITC for ME against Wild-Type and L/A and L/I Mutant Brd2 Bromodomains at 25 °C

bromodomain protein	K _d (nM)	ΔH (kcal/mol)
Brd2(1)	1470 ± 180	-8.6 ± 0.2
Brd2(1) _{L110I}	260 ± 40	-8.5 ± 0.1
Brd2(1) _{L110A}	17 ± 4	-16.8 ± 0.2
Brd2(2)	300 ± 80	-5.4 ± 0.1
Brd2(2) _{L383I}	27 ± 12	-9.8 ± 0.1
Brd2(2) _{L383A}	22 ± 4	-12.6 ± 0.1

highly potent against both leucine mutants, displaying K_d's of 17 and 22 nM against Brd2(1)_{L110A} and Brd2(2)_{L383A} and K_d's of 260 and 27 nM against Brd2(1)_{L110I} and Brd2(2)_{L383D}, respectively. Crucially, ME showed between 11-fold and 86-fold weaker affinities to WT compared with the leucine mutant proteins. As we anticipated, the diastereoisomer (±)-(1S,2S)-

16 did not induce a significant stabilization of mutant or WT proteins (Table 2).

Synthetic optimization of **ME** led to the highly potent and L/A mutant selective compound **ET** (**6**) (Figure 1C), data that we have reported elsewhere.¹¹ A complete binding selectivity profiling by DSF and ITC against all eight WT BET bromodomains and their L/A mutant counterparts showed that **ET** binds up to 540-fold more strongly and not less than 30-fold (average 160-fold) to L/A mutants compared with WT proteins, therefore validating our design strategy.¹¹ Importantly, selective targeting of engineered L/A mutants could be achieved in a cellular context, as demonstrated using a fluorescence recovery after photobleaching assay.¹¹

While indole derivative **28** could only induce moderate stabilization of W/F and W/H mutants, we noted that **28** greatly stabilized WT Brd2(1) and Brd2(2) (Table 2). We therefore decided to further characterize **28** and determined its binding affinity to Brd2(1) and Brd2(2) by ITC (Table 4).

Table 4. Binding Affinities (K_d 's, nM) of **28 Measured by ITC against Wild-Type First and Second Bromodomains of Brd2 and Brd4 and Compared with the K_d 's Reported for I-BET762 (**1**),¹¹ RVX-208 (**5**),^{10,38} MS436,³⁶ and Olinone³⁷**

bromodomain protein	I-BET762 (1) ¹¹	28	RVX-208 (5) ^{10,38}	MS436 ³⁶	olinone ³⁷
Brd2(1)	230	780	5800/16900		8600
Brd2(2)	100	45	250/206		>300000
Brd4(1)	95	520	1100/8930	85	3400
Brd4(2)	65	50	140/303	340	>300000

Compound **28** exhibited K_d 's of 800 and 40 nM against Brd2(1) and Brd2(2), respectively, corresponding to ca. 20-fold selectivity for the second over the first bromodomain. The same trend in selectivity was observed with the two bromodomains of Brd4 (Table 4). This selectivity of **28** for the second BET bromodomain could result at least in part from amino acid changes in the BC loop flanking the inhibitor binding site. In particular, an aspartate residue in the BC loop (Asp160 in Brd2(1)) is conserved among all first BET bromodomains and conservatively replaced by a histidine residue in the second BET bromodomains (His433 in Brd2(2), highlighted in Figure S1). To test this hypothesis, we solved the X-ray crystal structures of Brd2(2)_{W370F} in its apo form and with both **28** and the parent I-BET762 (**1**) bound (Figure 3, see Table S2 for X-ray crystallographic data collection and refinement statistics and Figure S2 for electron density map around the bound ligands). The binding modes of **28** and **1** to Brd2(2)_{W370F} were found to be identical, with all atoms of the triazolo-benzodiazepine scaffold superposing very well, and the aromatic indole ring of **28** being almost coplanar with the *para*-chloro-phenyl ring of **1** (Figure 3A). The observed binding mode recapitulates that of I-BET762/JQ1 bound to WT BET bromodomains, suggesting that it is not altered by the W/F mutation (Figure 3B). Importantly, the side chain of His433 switches from an "open" conformation observed in the crystal structure of Brd2(2)_{W370F} with **1** bound, pointing away from the ligand, to a "closed" conformation when **28** is bound to form an edge-to-face π stacking with the indole ring of **28** (Figure 3A). Both these "open" and "closed" histidine side chain conformers are observed in other crystal structures of wild-type C-terminal BET bromodomain, as in Brd2 (PDB codes 2E3K and 5BT5) and Brd3 (His395, PDB codes 2O01

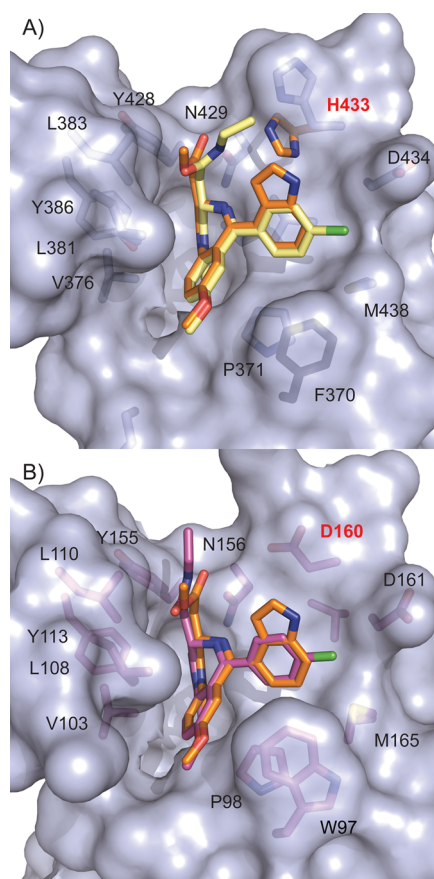


Figure 3. (A) Co-crystal structure of Brd2(2)_{W370F} (transparent surface representation) in complex with **28** (PDB code 5DFD, stick representation, orange carbons) superimposed with the cocystal structure of Brd2(2)_{W370F} in complex with I-BET762 (**1**) (PDB code 5DFC, stick representation, yellow carbons). The side chain of His433 switches from an "open" conformation when bound to **1** to a "closed" conformation when bound to **28**, engaging in an edge-to-face interaction with **28**. (B) Co-crystal structure of Brd2(1) in complex with **28** (PDB code 5DFD, stick representation, orange carbons) superimposed with the cocystal structure of Brd2(1) in complex with I-BET762 (**1**) (PDB code 2YEK,⁸ stick representation, pink carbons). All structures show a conserved scaffold binding mode in the K(Ac) pocket.

and 3S92). His433 in Brd2(2) is substituted by Asp160 in Brd2(1) (Figure 3B), which cannot engage in such an interaction in a closed conformation, potentially explaining the decreased potency of **28** against Brd2(1). Discrimination between first and second bromodomains of BET protein has been observed to varying degrees with small molecules RVX-208 (**5**),¹⁰ MS436,³⁶ and olinone³⁷ (Table 4), none of which are based on the triazolo-benzodiazepine scaffold. For example, RVX-208 (**5**) displayed up to 23-fold selectivity for Brd2(2) (K_d ca. 250 nM) compared with Brd2(1) (K_d ca. 5800 nM), which could also be explained by the flexibility of His433.³⁸ Our data highlight that such isoform selectivity can be achieved with the I-BET762/JQ1 scaffold via careful substitution of the parent chlorophenyl ring. This adds a useful isoform selectivity criterion that can be exploited for the design of next generation triazolo-benzodiazepine probes targeting BET proteins.

CONCLUSIONS

Here, we have described novel synthetic analogues of the triazolo-aryldiazepine-based bromodomain inhibitor I-BET762. We were able to introduce substitutions at the level of the methoxyphenyl ring, the ternary carbon center, the side chain methylene, and the chlorophenyl moiety. The design and development of the analogue series was aimed at targeting a number of specific BET bromodomain mutants with high selectivity compared with wild-type via a bump-and-hole approach. Among the “bumped” compounds reported, ME and ET achieved the highest selectivity levels targeting mutations at the Leu94 position.¹¹ Several interesting chemistries were developed in the process that will potentially see useful applications. For example, we showed that alkylation at the ternary center and the side chain methylene could be achieved, and that a high level of stereocontrol could be achieved during enolate alkylation. We also developed a new route allowing late stage diversity introduction at the level of the chlorophenyl ring. An indole analogue (28) was highly potent and displayed a marked BD2 selectivity profile by exploiting the aspartate/histidine substitution in the bromodomain BC loop. Taken together, we anticipate that our findings should be of broad interest, not only to other researchers working in the field of epigenetics and bromodomain inhibition but also to medicinal chemists focusing on related benzodiazepine systems.

ASSOCIATED CONTENT

Supporting Information

The Supporting Information is available free of charge on the ACS Publications website at DOI: 10.1021/acs.jmedchem.5b01135.

Material and methods, supplementary figures and tables, synthetic procedures, and characterization; purity of compounds (as measured by peak area ratio) was >95%, as determined by HPLC-MS (PDF)

SMILES representations of compounds 7–28 and ME (CSV)

Accession Codes

Coordinates for the X-ray structures of Brd2(2)_{W370F} apo and in complex with compounds 1 and 28 have been deposited in the Protein Data Bank (PDB) under accession codes SDFB, SDFC, and SDFD, respectively.

AUTHOR INFORMATION

Corresponding Author

*E-mail: a.ciulli@dundee.ac.uk

Present Addresses

^{||}M.G.J.B. Medical Research Council, Laboratory of Molecular Biology, Francis Crick Avenue, Cambridge Biomedical Campus, Cambridge CB2 0QH, U.K.

[†]E.L.S. Biochemistry and Molecular Biophysics Graduate Group, Perelman School of Medicine, University of Pennsylvania, Philadelphia, PA 19104, U.S.A.

[§]C.T. Nuffield Department of Clinical Medicine, Structural Genomics Consortium, University of Oxford, Old Road Campus, Roosevelt Drive, Oxford OX3 7DQ, U.K.

Notes

The authors declare no competing financial interest.

ACKNOWLEDGMENTS

This work was supported by awards to A.C. from the UK Biotechnology and Biological Sciences Research Council (BBSRC, Grants BB/J001201/1 and BB/J001201/2 and David Phillips Fellowship BB/G023123/1 and BB/G023123/2). E.L.S. was supported by a European Commission Erasmus work placement grant. Biophysics and drug discovery activities at Dundee are supported by a Wellcome Trust strategic award 100476/Z/12/Z to the Division of Biological Chemistry and Drug Discovery. We thank Stefan Knapp and his team at the Oxford Structural Genomics Consortium for providing expression vectors and the staff at the Diamond Light Source synchrotron for providing support on beamlines I02 and I03.

ABBREVIATIONS

ΔT_m , thermal shift; AcOH, acetic acid; ATP, adenosine triphosphate; BET, bromodomain and extra-terminal; Brd, bromodomain; DSF, differential scanning fluorimetry; FDA, Food and Drug Administration; ITC, isothermal titration calorimetry; K(Ac), acetyl-lysine; K_d , dissociation constant; NMR, nuclear magnetic resonance; NUT, nuclear protein in testis; THF, tetrahydrofuran; T_m , melting temperature; WT, wild-type

REFERENCES

- (1) Sternbach, L. H. The benzodiazepine story. *J. Med. Chem.* **1979**, *22*, 1–7.
- (2) Sternbach, L. H.; Fryer, R. I.; Metlesics, W.; Reeder, E.; Sach, G.; Saucy, G.; Stempel, A. Quinazolines and 1,4-Benzodiazepines. VI. 1a Halo-, Methyl-, and Methoxy-substituted 1,3-Dihydro-5-phenyl-2H-1,4-benzodiazepin-2-ones 1b,c. *J. Org. Chem.* **1962**, *27*, 3788–3796.
- (3) Sternbach, L. H. *The Benzodiazepines*; Raven Press: New York, 1973.
- (4) Ellman, J. A. Design, Synthesis, and Evaluation of Small-Molecule Libraries. *Acc. Chem. Res.* **1996**, *29*, 132–143.
- (5) Filippakopoulos, P.; Knapp, S. Targeting bromodomains: epigenetic readers of lysine acetylation. *Nat. Rev. Drug Discovery* **2014**, *13*, 337–356.
- (6) Nicodeme, E.; Jeffrey, K. L.; Schaefer, U.; Beinke, S.; Dewell, S.; Chung, C.; Chandwani, R.; Marazzi, I.; Wilson, P.; Coste, H.; White, J.; Kirilovsky, J.; Rice, C. M.; Lora, J. M.; Prinjha, R. K.; Lee, K.; Tarakhovskiy, A. Suppression of inflammation by a synthetic histone mimic. *Nature* **2010**, *468*, 1119–1123.
- (7) Filippakopoulos, P.; Qi, J.; Picaud, S.; Shen, Y.; Smith, W. B.; Fedorov, O.; Morse, E. M.; Keates, T.; Hickman, T. T.; Felletar, I.; Philpott, M.; Munro, S.; McKeown, M. R.; Wang, Y.; Christie, A. L.; West, N.; Cameron, M. J.; Schwartz, B.; Heightman, T. D.; La Thangue, N.; French, C. A.; Wiest, O.; Kung, A. L.; Knapp, S.; Bradner, J. E. Selective inhibition of BET bromodomains. *Nature* **2010**, *468*, 1067–1073.
- (8) Chung, C. W.; Coste, H.; White, J. H.; Mirguet, O.; Wilde, J.; Gosmini, R. L.; Delves, C.; Magny, S. M.; Woodward, R.; Hughes, S. A.; Boursier, E. V.; Flynn, H.; Bouillot, A. M.; Bamborough, P.; Brusq, J. M.; Gellibert, F. J.; Jones, E. J.; Riou, A. M.; Homes, P.; Martin, S. L.; Uings, I. J.; Toum, J.; Clement, C. A.; Boullay, A. B.; Grimley, R. L.; Blandel, F. M.; Prinjha, R. K.; Lee, K.; Kirilovsky, J.; Nicodeme, E. Discovery and characterization of small molecule inhibitors of the BET family bromodomains. *J. Med. Chem.* **2011**, *54*, 3827–3838.
- (9) Herait, P.; Dombret, H.; Thieblemont, C.; Facon, T.; Stathis, A.; Cunningham, D.; Palumbo, A.; Vey, N.; Michallet, M.; Recher, C.; Rezai, K.; Preudhomme, C. O7.3BET-bromodomain (BRD) inhibitor OTX015: Final results of the dose-finding part of a phase I study in hematologic malignancies. *Ann. Oncol.* **2015**, *26* (suppl2), ii10.
- (10) McLure, K. G.; Gesner, E. M.; Tsujikawa, L.; Kharenko, O. A.; Attwell, S.; Campeau, E.; Wasiak, S.; Stein, A.; White, A.; Fontano, E.;

Suto, R. K.; Wong, N. C.; Wagner, G. S.; Hansen, H. C.; Young, P. R. RVX-208, an Inducer of ApoA-I in Humans, Is a BET Bromodomain Antagonist. *PLoS One* **2013**, *8*, e83190.

(11) Baud, M. G. J.; Lin-Shiao, E.; Cardote, T.; Tallant, C.; Pschibul, A.; Chan, K.-H.; Zengerle, M.; Garcia, J. R.; Kwan, T. T. L.; Ferguson, F. M.; Ciulli, A. A Bump-and-Hole Approach to Engineer Controlled Selectivity of BET Bromodomain Chemical Probes. *Science* **2014**, *346*, 638–641.

(12) Prinjha, R. K.; Witherington, J.; Lee, K. Place your BETs: the therapeutic potential of bromodomains. *Trends Pharmacol. Sci.* **2012**, *33*, 146–153.

(13) A study to investigate the safety, pharmacokinetics, pharmacodynamics, and clinical activity of GSK525762 in subjects with NUT midline carcinoma (NMC). <https://clinicaltrials.gov/identifier/NCT01587703>.

(14) Delmore, J. E.; Issa, G. C.; Lemieux, M. E.; Rahl, P. B.; Shi, J.; Jacobs, H. M.; Kastriitis, E.; Gilpatrick, T.; Paranal, R. M.; Qi, J.; Chesi, M.; Schinzel, A. C.; McKeown, M. R.; Heffernan, T. P.; Vakoc, C. R.; Bergsagel, P. L.; Ghobrial, I. M.; Richardson, P. G.; Young, R. A.; Hahn, W. C.; Anderson, K. C.; Kung, A. L.; Bradner, J. E.; Mitsiades, C. S. BET Bromodomain Inhibition as a Therapeutic Strategy to Target c-Myc. *Cell* **2011**, *146*, 904–917.

(15) Dawson, M. A.; Prinjha, R. K.; Dittmann, A.; Giotopoulos, G.; Bantscheff, M.; Chan, W.; Robson, S. C.; Chung, C.; Hopf, C.; Savitski, M. M.; Huthmacher, C.; Gudgin, E.; Lugo, D.; Beinke, S.; Chapman, T. D.; Roberts, E. J.; Soden, P. E.; Auger, K. R.; Mirguet, O.; Doehner, K.; Delwel, R.; Burnett, A. K.; Jeffrey, P.; Drewes, G.; Lee, K.; Huntly, B. J. P.; Kouzarides, T. Inhibition of BET recruitment to chromatin as an effective treatment for MLL-fusion leukaemia. *Nature* **2011**, *478*, 529–533.

(16) Zuber, J.; Shi, J.; Wang, E.; Rappaport, A. R.; Herrmann, H.; Sison, E. A.; Magoon, D.; Qi, J.; Blatt, K.; Wunderlich, M.; Taylor, M. J.; Johns, C.; Chicas, A.; Mulloy, J. C.; Kogan, S. C.; Brown, P.; Valent, P.; Bradner, J. E.; Lowe, S. W.; Vakoc, C. R. RNAi screen identifies Brd4 as a therapeutic target in acute myeloid leukaemia. *Nature* **2011**, *478*, 524–528.

(17) Mertz, J. A.; Conery, A. R.; Bryant, B. M.; Sandy, P.; Balasubramanian, S.; Mele, D. A.; Bergeron, L.; Sims, R. J. Targeting MYC dependence in cancer by inhibiting BET bromodomains. *Proc. Natl. Acad. Sci. U. S. A.* **2011**, *108*, 16669–16674.

(18) Shah, K.; Liu, Y.; Deirmengian, C.; Shokat, K. M. Engineering unnatural nucleotide specificity for Rous sarcoma virus tyrosine kinase to uniquely label its direct substrates. *Proc. Natl. Acad. Sci. U. S. A.* **1997**, *94*, 3565–3570.

(19) Bishop, A. C.; Ubersax, J. A.; Petsch, D. T.; Matheos, D. P.; Gray, N. S.; Blethrow, J.; Shimizu, E.; Tsien, J. Z.; Schultz, P. G.; Rose, M. D.; Wood, J. L.; Morgan, D. O.; Shokat, K. M. A chemical switch for inhibitor-sensitive alleles of any protein kinase. *Nature* **2000**, *407*, 395–401.

(20) Dhalluin, C.; Carlson, J.; Zeng, L.; He, C.; Aggarwal, A.; Zhou, M. Structure and ligand of a histone acetyltransferase bromodomain. *Nature* **1999**, *399*, 491–496.

(21) Mujtaba, S.; He, Y.; Zeng, L.; Farooq, A.; Carlson, J.; Ott, M.; Verdin, E.; Zhou, M. Structural basis of lysine-acetylated HIV-1 Tat recognition by PCAF bromodomain. *Mol. Cell* **2002**, *9*, 575–586.

(22) Mujtaba, S.; He, Y.; Zeng, L.; Yan, S.; Plotnikova, O.; Sachchidanand; Sanchez, R.; Zeleznik-Le, N.; Ronai, Z.; Zhou, M. Structural mechanism of the bromodomain of the coactivator CBP in p53 transcriptional activation. *Mol. Cell* **2004**, *13*, 251–263.

(23) Huang, H.; Zhang, J.; Shen, W.; Wang, X.; Wu, J.; Wu, J.; Shi, Y. Solution structure of the second bromodomain of Brd2 and its specific interaction with acetylated histone tails. *BMC Struct. Biol.* **2007**, *7*, 57.

(24) Shen, W.; Xu, C.; Huang, W.; Zhang, J.; Carlson, J. E.; Tu, X.; Wu, J.; Shi, Y. Solution structure of human Brg1 bromodomain and its specific binding to acetylated histone tails. *Biochemistry* **2007**, *46* (8), 2100–2110.

(25) Liu, Y.; Wang, X.; Zhang, J.; Huang, H.; Ding, B.; Wu, J.; Shi, Y. Structural basis and binding properties of the second bromodomain of Brd4 with acetylated histone tails. *Biochemistry* **2008**, *47*, 6403–6417.

(26) Owen, D.; Ornaghi, P.; Yang, J.; Lowe, N.; Evans, P.; Ballario, P.; Neuhaus, D.; Filetici, P.; Travers, A. The structural basis for the recognition of acetylated histone H4 by the bromodomain of histone acetyltransferase gcn5p. *EMBO J.* **2000**, *19*, 6141–6149.

(27) Moriniere, J.; Rousseaux, S.; Steuerwald, U.; Soler-Lopez, M.; Curtet, S.; Vitte, A.-L.; Govin, J.; Gaucher, J.; Sadoul, K.; Hart, D. J.; Krijgsveld, J.; Khochbin, S.; Muller, C. W.; Petosa, C. Cooperative binding of two acetylation marks on a histone tail by a single bromodomain. *Nature* **2009**, *461*, 664–668.

(28) Jamieson, A. G.; Boutard, N.; Beauregard, K.; Bodas, M. S.; Ong, H.; Quiniou, C.; Chemtob, S.; Lubell, W. D. Positional Scanning for Peptide Secondary Structure by Systematic Solid-Phase Synthesis of Amino Lactam Peptides. *J. Am. Chem. Soc.* **2009**, *131*, 7917–7927.

(29) Carlier, P. R.; Zhao, H.; DeGuzman, J.; Lam, P. C. H. Enantioselective Synthesis of "Quaternary" 1,4-Benzodiazepin-2-one Scaffolds via Memory of Chirality. *J. Am. Chem. Soc.* **2003**, *125*, 11482–11483.

(30) Carlier, P. R.; Lam, P. C. H.; DeGuzman, J. C.; Zhao, H. Memory of Chirality Trapping of Low Inversion Barrier 1,4-benzodiazepin-2-one Enolates. *Tetrahedron: Asymmetry* **2005**, *16*, 2998–3002.

(31) Carlier, P. R.; Zhao, H.; MacQuarrie-Hunter, S. L.; DeGuzman, J. C.; Hsu, D. C. Enantioselective Synthesis of Diversely Substituted Quaternary 1,4-Benzodiazepine-2,5-diones. *J. Am. Chem. Soc.* **2006**, *128*, 15215–15220.

(32) Nadin, A.; Sanchez Lopez, J. M.; Owens, A. P.; Howells, D. M.; Talbot, A. C.; Harrison, T. New Synthesis of 1,3-Dihydro-1,4-benzodiazepin-2(2H)-ones and 3-Amino-1,3-Dihydro-1,4-benzodiazepin-2(2H)-ones: Pd-Catalysed Cross-Coupling of Imidoyl Chlorides with Organoboronic Acids. *J. Org. Chem.* **2003**, *68*, 2844–2852.

(33) Carter, M. C.; Alber, D. G.; Baxter, R. C.; Bithell, S. K.; Budworth, J.; Chubb, A.; Cockerill, G. S.; Dowdell, V. C. L.; Henderson, E. A.; Keegan, S. J.; Kelsey, R. D.; Lockyer, M. J.; Stables, J. N.; Wilson, L. J.; Powell, K. L. 1,4-Benzodiazepines as Inhibitors of Respiratory Syncytial Virus. *J. Med. Chem.* **2006**, *49*, 2311–2319.

(34) Hitotsuyanagi, Y.; Motegi, S.; Fukaya, H.; Takeya, K. A cis Amide Bond Surrogate Incorporating 1,2,4-Triazole. *J. Org. Chem.* **2002**, *67*, 3266–3271.

(35) Syeda, S. S.; Jakkaraj, S.; Georg, G. I. Scalable syntheses of the BET bromodomain inhibitor JQ1. *Tetrahedron Lett.* **2015**, *56*, 3454–3457.

(36) Zhang, G.; Plotnikov, A. N.; Rusinova, E.; Shen, T.; Morohashi, K.; Joshua, J.; Zeng, L.; Mujtaba, S.; Ohlmeyer, M.; Zhou, M.-M. Structure-Guided Design of Potent Diazobenzene Inhibitors for the BET Bromodomains. *J. Med. Chem.* **2013**, *56*, 9251–9264.

(37) Gacias, M.; Gerona-Navarro, G.; Plotnikov, A. N.; Zhang, G.; Zeng, L.; Kaur, J.; Moy, G.; Rusinova, E.; Rodriguez, Y.; Matikainen, B.; Vincek, A.; Joshua, J.; Casaccia, P.; Zhou, M.-M. Selective Chemical Modulation of Gene Transcription Favours Oligodendrocyte Lineage Progression. *Chem. Biol.* **2014**, *21*, 841–854.

(38) Picaud, S.; Wells, C.; Felletar, I.; Brotherton, D.; Martin, S.; Savitsky, P.; Diez-Dacal, B.; Philpott, M.; Bountra, C.; Lingard, H.; Fedorov, O.; Müller, S.; Brennan, P. E.; Knapp, S.; Filippakopoulos, P. RVX-208, an inhibitor of BET transcriptional regulators with selectivity for the second bromodomain. *Proc. Natl. Acad. Sci. U. S. A.* **2013**, *110*, 19754–19759.